

Supporting Information for

Alkane guest packing drives switching between multimeric deep-cavity cavitand host assembly states

J. Wesley Barnett^a, Du Tang^a, Bruce C. Gibb,^b and Henry S. Ashbaugh^{*b}

^aDepartment of Chemical and Biomolecular Engineering, Tulane University, New Orleans, LA, 70118

^bDepartment of Chemistry, Tulane University, New Orleans, LA, 70118

In this supplement we provide full details for the simulations of alkane transfer into multimeric TEMOA complexes and present the simulation results for guest transfer into octameric cavitands.

Molecular Simulation and Computational Methods. Molecular dynamics simulations of linear alkane guests encapsulated within multimeric TEMOA complexes in water were performed using GROMACS 5.05.¹ Water was modeled using the TIP4P/EW force-field², which provides an excellent description of the structure and thermodynamics of liquid properties of liquid water near ambient conditions. TEMOA Lennard-Jones and intramolecular interactions were modeled using the General Amber Force Field (GAFF).³ ACPYPE⁴ was used to assign AM1-BCC⁵ partial charges. Following previously reported calculations, the net charge on each host was set to $-6e$ at neutral pH.⁶ Specifically, the four carboxylic acid coating groups ringing each host's hydrophobic pocket and two acids diagonal to one another at the foot of OA were deprotonated. Six sodium counter cations, modeled using the GAFF potential, were added for each host to neutralize the host/guest complexes. Figure S1 shows a snapshot of a single octa-acid host rendered using the coordinates reported in Table S1 in standard Protein Data Bank format. Table S2 lists the partial charges and non-bonded GAFF atom types used to model the

host electrostatic and Lennard-Jones interactions. Alkane guests were modeled using the L-OPLS force-field.⁷ The L-OPLS force-field for the alkanes was chosen over the GAFF or OPLS force-fields because L-OPLS provides a more accurate representation of the conformational equilibrium of the alkanes of increasing length. This is especially important here for the range of guest sizes considered here. This model for cavitands in water conforms to that we previously used successfully to examine conformational equilibrium of alkanes within dimeric OA capsules and the non-monotonic assembly of monomeric and dimeric cavitand complexes with alkanes, giving us confidence in the simulations reported here. Lennard-Jones cross interactions were evaluated using Lorentz-Berthelot combining rules.⁸ Lennard-Jones interactions were cut-off beyond 9 Å with a mean-field correction for longer-range contributions. Long-range electrostatic interactions were evaluated using particle-mesh Ewald summation with a real-space cut-off beyond 9 Å.⁹ Host-guest complexes were hydrated by anywhere from 3,500 to 12,500 waters depending on the size of the complex (dimer, tetramer, hexamer, or octamer). The number of alkane guests within the TEMOA complex was one, two, three, or four for the dimeric, tetrameric, hexameric, octameric complexes, respectively, to maintain a two-to-one host/guest ratio as determined experimentally. Simulations were performed in the isothermal-isobaric ensemble at 25°C and 1 bar. The temperature and pressure were maintained using the Nosé-Hoover thermostat¹⁰ and Parinello-Rahman barostat,¹¹ respectively. Bonds involving hydrogens for the hosts and guests were constrained using the LINCS algorithm,¹² while water was held rigid using SETTLE.¹³ The equations-of-motion were integrated with a time step of 2 fs.

We assessed the impact of alkane guest packing on the relative stability of multimeric TEMOA complexes from the free energy of transferring guests from vacuum into the complex interior. Transfer free energies were evaluated for alkanes C₁ to C₁₈ into dimeric complexes, C₁

to C₂₆ into tetrameric complexes, C₁ to C₃₂ into hexameric complexes, and C₁ to C₃₂ into octameric complexes. One, two, three, or four guests were simultaneously grown into each complex to maintain a two-to-one host/guest ratio. Incremental free energy differences between guests with $n-1$ to n carbon units were evaluated using the Multistate Bennett Acceptance Ratio technique.¹⁴ Free energy increments were evaluated using a coupling-parameter approach to evaluate Lennard-Jones and electrostatic contributions to the free energy over four simulation phases. In the first phase, the charges on a terminal methyl of the $n-1$ carbon alkane were turned off in 0.25 λ increments from 1 to 0, where 1 indicates full interactions and 0 indicates no interactions. In the second phase, the new terminal methyl group van der Waals interactions of the n alkane were turned on in 0.05 λ increments. In the third phase, the electrostatic interactions of the methylene adjacent to the new terminal methyl unit were turned on in 0.25 λ increments, while in the fourth phase the electrostatic interactions of the methyl unit were turned on in 0.25 λ increments. Each intermediate state in the growth process was simulated for 5 ns to evaluate averages following 1 ns for equilibration. Since the host complexes are only stable experimentally over specific ranges of guest lengths, it was necessary to stabilize the simulated complexes using harmonic restraints to keep them from falling apart during the guest growth process. To this end, host complexes were assembled to form a dimer, tetramer, hexamer, or octamer with restraints applied between the carbons touching neighboring hosts in the complexes were applied with a spring constant of 150 kJ/mol and bond length of 3.4 Å. The constituent host portals for the tetrameric, hexameric, and octameric complexes were placed on the faces of a tetrahedral, cubic, or octahedral Platonic solid.

The internal volumes of the empty complexes and van der Waals volumes of the guests was determined using Monte Carlo integration. The internalized volume was evaluated by

randomly inserting 10^5 points into a box bounding the empty multimer complexes averaged over 25,000 simulation snapshots. The volume from a single simulation snapshot was determined by the fraction of points inside the complex's internal guest-hosting cavity bound by the van der Waals volume of the cavitands. The van der Waals volumes of the *n*-alkanes was determined by performing 10^5 insertions over a bounding box containing the guest in the fully extended all trans conformation. The van der Waals radii of the hydrogen, carbon, and oxygen units were assumed to be 1.2 Å, 1.7 Å, and 1.5 Å, respectively, as reported by Bondi. In the case of the octamer, the host complex collapsed as the guest length decreased and retreated to single host pockets making determination of the internalized volume difficult. We therefore used a geometric model to evaluate the volume of the octamer as described below.

Guest Transfer into Octameric Host Complexes. In Figure S2 we compare the free energies of transferring alkanes from vacuum into the interiors of a hexameric and octameric TEMOA complexes. For short chains the transfer free energy into the octamer closely tracks that of the hexamer, and by extension the dimer and tetramer (Figure 2). The transfer free energy into the hexamer drops significantly below that of the octamer beginning around C₁₆, soon after which transfer into the hexamer is favored over than of the dimer and tetramer beginning with C₁₉ (Figure 2). The hexamer transfer free energy reaches a minimum for C₂₆, after which it increases with increasing guest length. The hexamer transfer free energy crosses that for the octamer for alkanes between C₂₈ and C₂₉, after which the octamer has the lowest free energy. We therefore anticipate the octamer would be stabilized by guests transfer for alkanes C₂₉ and longer.

We note that while the empty dimer, tetramer, and hexamer complexes were stable and rigid, the empty octameric complex was unstable and collapsed even though the touching edges

of the complex were harmonically restrained. As a result the excess volume of the empty octamer was negligible, on the order of $\sim 100 \text{ \AA}^3$. The internalized volume of the octamer swelled considerably as the guests were added, while those of the other, more rigid, complexes were not as sensitive to guest addition. This makes unambiguous determination of the octamer volume difficult following the Monte Carlo procedure described above. Progress can be made, however, if we consider the shapes of the excess volumes of the hexamer and octamer. In the case of the hexamer the excess volume is a cube with side length D , the diameter of the circular projection of TEMOA onto the face of excess volume. For a cubic excess volume of $V_{ex}(\text{hexamer}) = D^3 = 2259 \text{ \AA}^3$, we determine the effective circular diameter of the TEMOA to be $D = (2259 \text{ \AA}^3)^{1/3} = 13.1 \text{ \AA}$. In the case of the octamer, the excess volume is an octahedron with equilateral triangular faces. The side length of an equilateral triangle within which a circle of diameter D can be inscribed is $\sqrt{3}D$. The corresponding volume of an octahedron with edges of length $\sqrt{3}D$ is $V_{ex}(\text{octamer}) = \sqrt{6}D^3 = \sqrt{6}V_{ex}(\text{hexamer}) = 5533 \text{ \AA}^3$. The total internalized volume of the octamer is subsequently $V_{tot}(\text{octamer}) = V_{ex}(\text{octamer}) + 4V_{tot}(\text{dimer}) = 7881 \text{ \AA}^3$. In Figure S3 we plot the guest packing fraction for four alkanes within the interior of the octamer as a function of the number of carbons in a single chain. This line crosses a packing fraction of $\eta = 0.25$ between C_{28} and C_{29} , leading us to anticipate from the empirical correlation described in the paper that guests prefer transfer into the octamer for guests C_{29} and longer. This prediction is in good agreement with the simulation results determined from the guest transfer free energies reported in Figure S2. Extrapolating the octamer packing fraction beyond the range of guests simulated, we find it crosses $\eta = 0.30$ between C_{34} and C_{35} (Figure S3). We anticipate from this comparison then that we would not expect octamers to be observed experimentally until the guests C_{35} and longer. The melting point of C_{35} is 75°C , challenging preparation of these host/guest complexes following

the previously used experimental procedures as a result of the increased volatility of the aqueous solution.

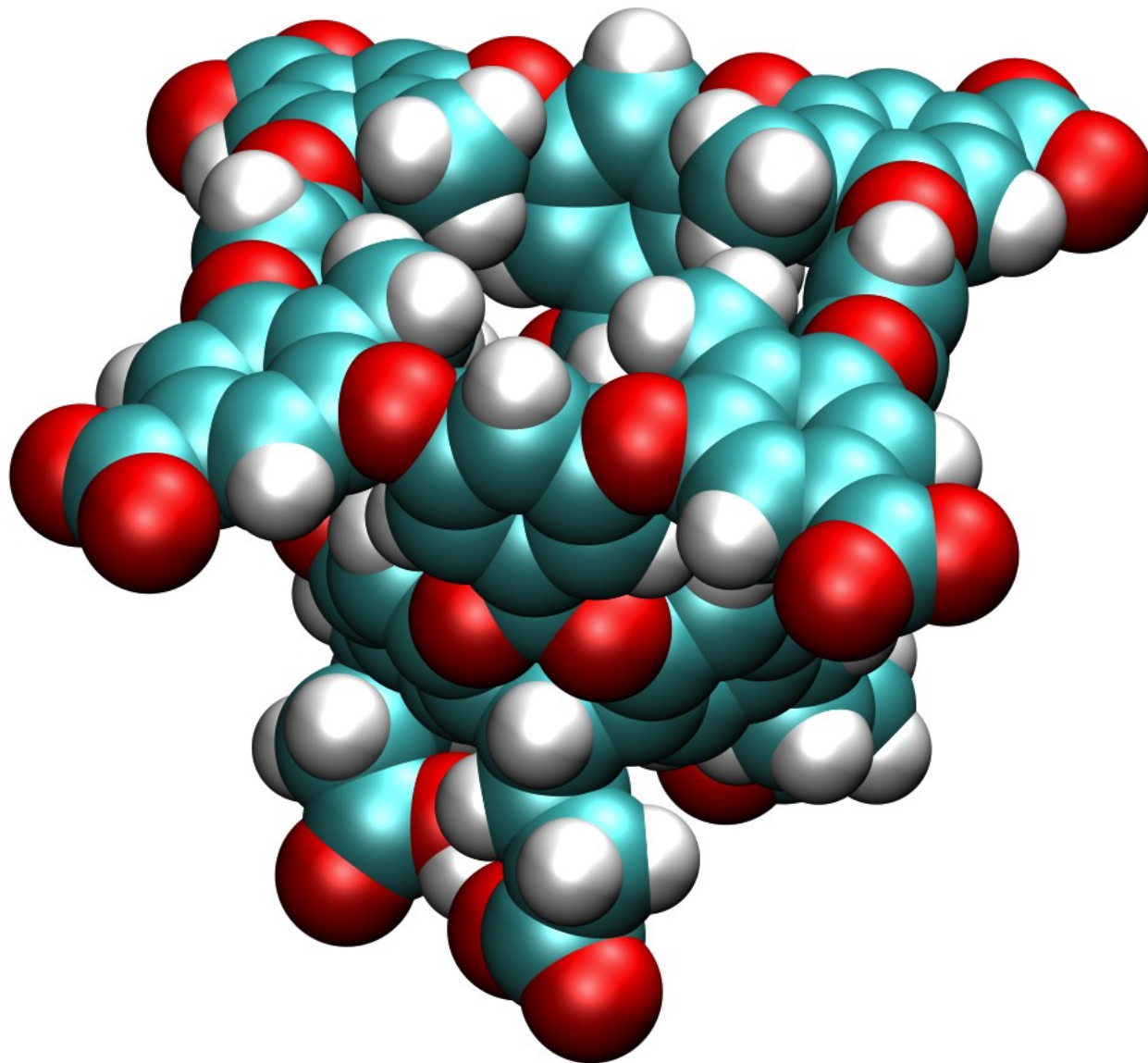


Figure S1. Snapshot of a single TEMOA cavitand from the simulations performed here. Protein data bank structure reported in Table S1. Partial charges and GAFF atom types reported in Table S2.

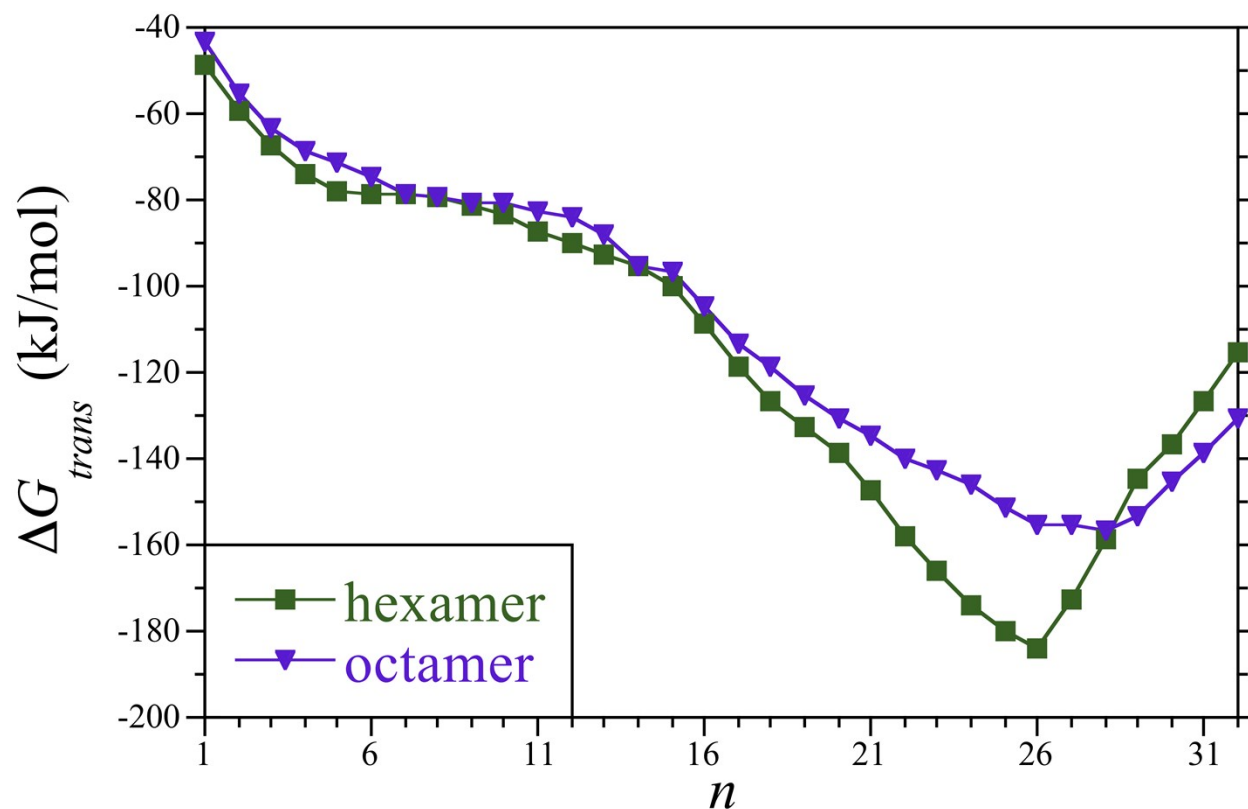


Figure S2. Vacuum-to-complex transfer free energies into the hexameric and octameric complexes for alkane guests as a function of the number of guest carbons. Error bars are smaller than the figure symbols. While $n_g = 3$ or 4 guests were transferred into the hexamer and octamer complexes, respectively, the transfer free energies are reported on a per guest basis to affect a proper comparison. The octamer transfer free energy crosses that for the hexamer between C_{28} and C_{29} .

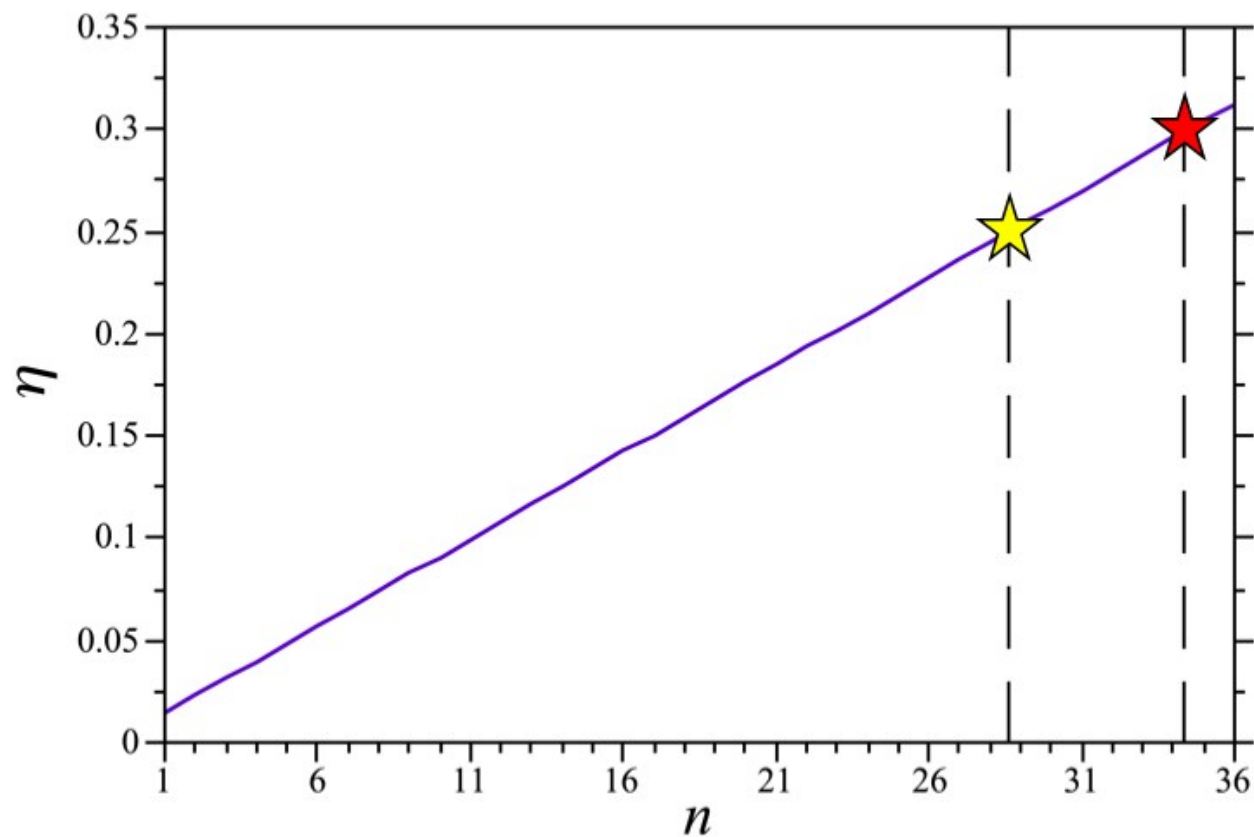


Figure S3. Packing fraction of alkane guests within octameric complex as a function of the number of guest carbons. The yellow star indicates the guest size at which $\eta = 0.25$, where we anticipate the vacuum-to-complex transfer free energy would favor the octameric complex. The red star indicates at which $\eta = 0.30$, where we anticipate the complex would be stabilized in solution following the correlation developed for the smaller complexes in the paper.

Table S1. Protein data bank structure of a single TEMOA host illustrated in Figure S1.

TITLE	TEMOA								
AUTHOR	J.W.BARNETT								
CRYST1	17.968	17.485	13.147	90.00	90.00	90.00	P 1		1
MODEL	1								
ATOM	1	O1	MOL	1	-1.740	-4.920	7.500	1.00	0.00
ATOM	2	C1	MOL	1	-1.360	-4.170	6.650	1.00	0.00
ATOM	3	O2	MOL	1	-1.630	-2.890	6.590	1.00	0.00
ATOM	4	H1	MOL	1	-2.370	-2.560	7.140	1.00	0.00
ATOM	5	C2	MOL	1	-0.550	-4.650	5.450	1.00	0.00
ATOM	6	H2	MOL	1	-0.120	-5.610	5.720	1.00	0.00
ATOM	7	H3	MOL	1	-1.310	-4.860	4.700	1.00	0.00
ATOM	8	C3	MOL	1	0.510	-3.700	4.880	1.00	0.00
ATOM	9	H4	MOL	1	1.490	-4.010	5.230	1.00	0.00
ATOM	10	H5	MOL	1	0.350	-2.710	5.280	1.00	0.00
ATOM	11	C4	MOL	1	0.540	-3.680	3.330	1.00	0.00
ATOM	12	H6	MOL	1	0.670	-4.700	3.000	1.00	0.00
ATOM	13	C5	MOL	1	1.730	-2.890	2.760	1.00	0.00
ATOM	14	C6	MOL	1	2.270	-1.760	3.380	1.00	0.00
ATOM	15	H7	MOL	1	1.880	-1.460	4.330	1.00	0.00
ATOM	16	C7	MOL	1	-0.760	-3.170	2.710	1.00	0.00
ATOM	17	C8	MOL	1	-1.550	-2.200	3.330	1.00	0.00
ATOM	18	H8	MOL	1	-1.240	-1.840	4.280	1.00	0.00
ATOM	19	C9	MOL	1	-2.730	-1.710	2.790	1.00	0.00
ATOM	20	C10	MOL	1	-3.570	-0.650	3.530	1.00	0.00
ATOM	21	C11	MOL	1	-3.500	-0.900	5.050	1.00	0.00
ATOM	22	C12	MOL	1	-4.550	-0.230	5.930	1.00	0.00
ATOM	23	C13	MOL	1	-4.540	-0.760	7.390	1.00	0.00
ATOM	24	O3	MOL	1	-5.370	-0.250	8.130	1.00	0.00
ATOM	25	O4	MOL	1	-3.710	-1.650	7.680	1.00	0.00
ATOM	26	H9	MOL	1	-5.550	-0.390	5.540	1.00	0.00
ATOM	27	H10	MOL	1	-4.410	0.850	5.970	1.00	0.00
ATOM	28	H11	MOL	1	-3.610	-1.970	5.180	1.00	0.00
ATOM	29	H12	MOL	1	-2.520	-0.670	5.440	1.00	0.00
ATOM	30	H13	MOL	1	-4.590	-0.800	3.210	1.00	0.00
ATOM	31	C14	MOL	1	-3.150	0.730	3.020	1.00	0.00
ATOM	32	C15	MOL	1	-2.140	1.480	3.610	1.00	0.00
ATOM	33	H14	MOL	1	-1.700	1.100	4.510	1.00	0.00
ATOM	34	C16	MOL	1	-1.640	2.660	3.070	1.00	0.00
ATOM	35	C17	MOL	1	-0.420	3.400	3.660	1.00	0.00
ATOM	36	H15	MOL	1	-0.540	4.440	3.390	1.00	0.00
ATOM	37	C18	MOL	1	-0.380	3.320	5.200	1.00	0.00
ATOM	38	H16	MOL	1	-1.270	3.830	5.560	1.00	0.00
ATOM	39	C19	MOL	1	0.880	3.920	5.860	1.00	0.00
ATOM	40	H17	MOL	1	0.590	4.660	6.620	1.00	0.00
ATOM	41	H18	MOL	1	1.510	4.450	5.160	1.00	0.00
ATOM	42	C20	MOL	1	1.730	2.880	6.590	1.00	0.00
ATOM	43	O5	MOL	1	1.280	1.830	6.950	1.00	0.00
ATOM	44	O6	MOL	1	2.960	3.270	6.780	1.00	0.00
ATOM	45	H19	MOL	1	3.550	2.540	7.070	1.00	0.00
ATOM	46	H20	MOL	1	-0.460	2.310	5.550	1.00	0.00
ATOM	47	C21	MOL	1	0.850	2.930	2.940	1.00	0.00
ATOM	48	C22	MOL	1	1.660	1.910	3.440	1.00	0.00
ATOM	49	H21	MOL	1	1.370	1.440	4.360	1.00	0.00
ATOM	50	C23	MOL	1	2.820	1.480	2.800	1.00	0.00

ATOM	51	C24	MOL	1	3.700	0.380	3.390	1.00	0.00
ATOM	52	H22	MOL	1	4.700	0.560	3.000	1.00	0.00
ATOM	53	C25	MOL	1	3.800	0.520	4.920	1.00	0.00
ATOM	54	H23	MOL	1	3.890	1.570	5.110	1.00	0.00
ATOM	55	C26	MOL	1	4.990	-0.150	5.600	1.00	0.00
ATOM	56	H24	MOL	1	5.900	0.030	5.030	1.00	0.00
ATOM	57	H25	MOL	1	4.880	-1.230	5.660	1.00	0.00
ATOM	58	C27	MOL	1	5.270	0.370	7.040	1.00	0.00
ATOM	59	O7	MOL	1	4.730	1.440	7.390	1.00	0.00
ATOM	60	O8	MOL	1	6.060	-0.310	7.690	1.00	0.00
ATOM	61	H26	MOL	1	2.880	0.210	5.410	1.00	0.00
ATOM	62	C28	MOL	1	3.250	-0.960	2.800	1.00	0.00
ATOM	63	C29	MOL	1	3.720	-1.340	1.550	1.00	0.00
ATOM	64	O9	MOL	1	4.620	-0.580	0.850	1.00	0.00
ATOM	65	C30	MOL	1	3.250	-2.480	0.930	1.00	0.00
ATOM	66	H27	MOL	1	3.630	-2.770	-0.030	1.00	0.00
ATOM	67	C31	MOL	1	2.250	-3.240	1.520	1.00	0.00
ATOM	68	O10	MOL	1	1.780	-4.310	0.810	1.00	0.00
ATOM	69	C32	MOL	1	0.610	-4.090	0.070	1.00	0.00
ATOM	70	H28	MOL	1	0.490	-3.030	-0.070	1.00	0.00
ATOM	71	O11	MOL	1	-0.500	-4.580	0.770	1.00	0.00
ATOM	72	C33	MOL	1	-1.210	-3.650	1.480	1.00	0.00
ATOM	73	C34	MOL	1	-2.370	-3.170	0.910	1.00	0.00
ATOM	74	H29	MOL	1	-2.690	-3.550	-0.040	1.00	0.00
ATOM	75	C35	MOL	1	-3.120	-2.200	1.550	1.00	0.00
ATOM	76	O12	MOL	1	-4.240	-1.740	0.920	1.00	0.00
ATOM	77	C36	MOL	1	-4.130	-0.500	0.290	1.00	0.00
ATOM	78	H30	MOL	1	-3.080	-0.310	0.110	1.00	0.00
ATOM	79	O13	MOL	1	-4.620	0.510	1.110	1.00	0.00
ATOM	80	C37	MOL	1	-3.680	1.220	1.830	1.00	0.00
ATOM	81	C38	MOL	1	-3.250	2.410	1.290	1.00	0.00
ATOM	82	H31	MOL	1	-3.670	2.770	0.380	1.00	0.00
ATOM	83	C39	MOL	1	-2.220	3.110	1.890	1.00	0.00
ATOM	84	O14	MOL	1	-1.780	4.250	1.250	1.00	0.00
ATOM	85	C40	MOL	1	-0.640	4.090	0.460	1.00	0.00
ATOM	86	H32	MOL	1	-0.530	3.040	0.220	1.00	0.00
ATOM	87	O15	MOL	1	0.490	4.510	1.150	1.00	0.00
ATOM	88	C41	MOL	1	1.230	3.520	1.740	1.00	0.00
ATOM	89	C42	MOL	1	2.370	3.100	1.080	1.00	0.00
ATOM	90	H33	MOL	1	2.650	3.560	0.150	1.00	0.00
ATOM	91	C43	MOL	1	3.140	2.080	1.600	1.00	0.00
ATOM	92	O16	MOL	1	4.230	1.680	0.870	1.00	0.00
ATOM	93	C44	MOL	1	4.090	0.500	0.140	1.00	0.00
ATOM	94	H34	MOL	1	3.030	0.320	-0.010	1.00	0.00
ATOM	95	C45	MOL	1	4.730	0.640	-1.230	1.00	0.00
ATOM	96	C46	MOL	1	4.710	1.880	-1.850	1.00	0.00
ATOM	97	H35	MOL	1	4.410	2.750	-1.320	1.00	0.00
ATOM	98	C47	MOL	1	5.150	-0.500	-1.900	1.00	0.00
ATOM	99	H36	MOL	1	5.190	-1.450	-1.400	1.00	0.00
ATOM	100	C48	MOL	1	5.530	-0.390	-3.230	1.00	0.00
ATOM	101	O17	MOL	1	5.950	-1.430	-3.990	1.00	0.00
ATOM	102	C49	MOL	1	5.510	0.840	-3.870	1.00	0.00
ATOM	103	H37	MOL	1	5.790	0.910	-4.900	1.00	0.00
ATOM	104	C50	MOL	1	5.100	1.970	-3.180	1.00	0.00
ATOM	105	O18	MOL	1	5.100	3.110	-3.910	1.00	0.00
ATOM	106	C51	MOL	1	4.510	4.290	-3.490	1.00	0.00
ATOM	107	C52	MOL	1	5.340	5.330	-3.120	1.00	0.00

ATOM	108	C53	MOL	1	4.830	6.590	-2.870	1.00	0.00
ATOM	109	C54	MOL	1	3.450	6.780	-2.980	1.00	0.00
ATOM	110	H38	MOL	1	3.040	7.760	-2.810	1.00	0.00
ATOM	111	C55	MOL	1	5.770	7.790	-2.570	1.00	0.00
ATOM	112	O19	MOL	1	5.200	8.870	-2.400	1.00	0.00
ATOM	113	O20	MOL	1	6.970	7.520	-2.560	1.00	0.00
ATOM	114	H39	MOL	1	6.400	5.170	-3.060	1.00	0.00
ATOM	115	C56	MOL	1	3.130	4.460	-3.640	1.00	0.00
ATOM	116	C57	MOL	1	2.240	3.360	-4.150	1.00	0.00
ATOM	117	H40	MOL	1	2.800	2.690	-4.800	1.00	0.00
ATOM	118	H41	MOL	1	1.400	3.770	-4.710	1.00	0.00
ATOM	119	H42	MOL	1	1.830	2.760	-3.340	1.00	0.00
ATOM	120	C58	MOL	1	2.630	5.740	-3.350	1.00	0.00
ATOM	121	O21	MOL	1	1.310	6.030	-3.630	1.00	0.00
ATOM	122	C59	MOL	1	0.260	5.670	-2.850	1.00	0.00
ATOM	123	C60	MOL	1	-0.980	5.800	-3.440	1.00	0.00
ATOM	124	H43	MOL	1	-1.060	6.160	-4.450	1.00	0.00
ATOM	125	C61	MOL	1	0.380	5.200	-1.550	1.00	0.00
ATOM	126	H44	MOL	1	1.340	5.110	-1.080	1.00	0.00
ATOM	127	C62	MOL	1	-0.780	4.840	-0.860	1.00	0.00
ATOM	128	C63	MOL	1	-2.030	4.970	-1.440	1.00	0.00
ATOM	129	H45	MOL	1	-2.920	4.710	-0.900	1.00	0.00
ATOM	130	C64	MOL	1	-2.120	5.450	-2.740	1.00	0.00
ATOM	131	O22	MOL	1	-3.290	5.610	-3.410	1.00	0.00
ATOM	132	C65	MOL	1	-4.470	4.970	-3.090	1.00	0.00
ATOM	133	C66	MOL	1	-5.510	5.750	-2.620	1.00	0.00
ATOM	134	C67	MOL	1	-6.770	5.200	-2.440	1.00	0.00
ATOM	135	C68	MOL	1	-6.940	3.850	-2.700	1.00	0.00
ATOM	136	H46	MOL	1	-7.920	3.410	-2.570	1.00	0.00
ATOM	137	C69	MOL	1	-7.970	6.090	-2.030	1.00	0.00
ATOM	138	O23	MOL	1	-7.700	7.280	-1.860	1.00	0.00
ATOM	139	O24	MOL	1	-9.050	5.510	-1.950	1.00	0.00
ATOM	140	H47	MOL	1	-5.360	6.790	-2.430	1.00	0.00
ATOM	141	C70	MOL	1	-4.630	3.620	-3.400	1.00	0.00
ATOM	142	C71	MOL	1	-3.520	2.810	-4.020	1.00	0.00
ATOM	143	H48	MOL	1	-3.930	2.040	-4.660	1.00	0.00
ATOM	144	H49	MOL	1	-2.900	2.320	-3.270	1.00	0.00
ATOM	145	H50	MOL	1	-2.870	3.440	-4.610	1.00	0.00
ATOM	146	C72	MOL	1	-5.890	3.080	-3.160	1.00	0.00
ATOM	147	O25	MOL	1	-6.170	1.790	-3.560	1.00	0.00
ATOM	148	C73	MOL	1	-5.720	0.680	-2.920	1.00	0.00
ATOM	149	C74	MOL	1	-5.720	-0.480	-3.670	1.00	0.00
ATOM	150	H51	MOL	1	-6.050	-0.460	-4.690	1.00	0.00
ATOM	151	C75	MOL	1	-5.280	0.680	-1.600	1.00	0.00
ATOM	152	H52	MOL	1	-5.290	1.580	-1.020	1.00	0.00
ATOM	153	C76	MOL	1	-4.830	-0.520	-1.050	1.00	0.00
ATOM	154	C77	MOL	1	-4.840	-1.700	-1.790	1.00	0.00
ATOM	155	H53	MOL	1	-4.510	-2.620	-1.350	1.00	0.00
ATOM	156	C78	MOL	1	-5.280	-1.670	-3.100	1.00	0.00
ATOM	157	O26	MOL	1	-5.310	-2.740	-3.930	1.00	0.00
ATOM	158	C79	MOL	1	-4.700	-3.950	-3.650	1.00	0.00
ATOM	159	C80	MOL	1	-5.520	-5.020	-3.330	1.00	0.00
ATOM	160	C81	MOL	1	-5.000	-6.300	-3.210	1.00	0.00
ATOM	161	C82	MOL	1	-3.640	-6.470	-3.400	1.00	0.00
ATOM	162	H54	MOL	1	-3.220	-7.460	-3.330	1.00	0.00
ATOM	163	C83	MOL	1	-5.930	-7.520	-2.980	1.00	0.00
ATOM	164	O27	MOL	1	-7.130	-7.250	-2.890	1.00	0.00

ATOM	165	O28	MOL	1	-5.360	-8.610	-2.940	1.00	0.00
ATOM	166	H55	MOL	1	-6.580	-4.870	-3.210	1.00	0.00
ATOM	167	C84	MOL	1	-3.340	-4.110	-3.870	1.00	0.00
ATOM	168	C85	MOL	1	-2.470	-2.960	-4.320	1.00	0.00
ATOM	169	H56	MOL	1	-1.660	-3.320	-4.950	1.00	0.00
ATOM	170	H57	MOL	1	-2.020	-2.440	-3.480	1.00	0.00
ATOM	171	H58	MOL	1	-3.050	-2.240	-4.880	1.00	0.00
ATOM	172	C86	MOL	1	-2.830	-5.400	-3.720	1.00	0.00
ATOM	173	O29	MOL	1	-1.520	-5.670	-4.080	1.00	0.00
ATOM	174	C87	MOL	1	-0.440	-5.380	-3.310	1.00	0.00
ATOM	175	C88	MOL	1	0.780	-5.450	-3.970	1.00	0.00
ATOM	176	H59	MOL	1	0.810	-5.720	-5.010	1.00	0.00
ATOM	177	C89	MOL	1	-0.490	-5.020	-1.970	1.00	0.00
ATOM	178	H60	MOL	1	-1.430	-4.980	-1.460	1.00	0.00
ATOM	179	C90	MOL	1	0.690	-4.720	-1.310	1.00	0.00
ATOM	180	C91	MOL	1	1.920	-4.800	-1.950	1.00	0.00
ATOM	181	H61	MOL	1	2.830	-4.590	-1.430	1.00	0.00
ATOM	182	C92	MOL	1	1.950	-5.160	-3.290	1.00	0.00
ATOM	183	O30	MOL	1	3.080	-5.270	-4.030	1.00	0.00
ATOM	184	C93	MOL	1	4.280	-4.650	-3.710	1.00	0.00
ATOM	185	C94	MOL	1	5.340	-5.460	-3.360	1.00	0.00
ATOM	186	H62	MOL	1	5.200	-6.520	-3.260	1.00	0.00
ATOM	187	C95	MOL	1	4.420	-3.280	-3.910	1.00	0.00
ATOM	188	C96	MOL	1	3.280	-2.420	-4.400	1.00	0.00
ATOM	189	H63	MOL	1	2.600	-3.000	-5.010	1.00	0.00
ATOM	190	H64	MOL	1	3.660	-1.590	-4.990	1.00	0.00
ATOM	191	H65	MOL	1	2.700	-2.000	-3.580	1.00	0.00
ATOM	192	C97	MOL	1	5.690	-2.760	-3.690	1.00	0.00
ATOM	193	C98	MOL	1	6.770	-3.560	-3.350	1.00	0.00
ATOM	194	H66	MOL	1	7.750	-3.130	-3.240	1.00	0.00
ATOM	195	C99	MOL	1	6.610	-4.920	-3.200	1.00	0.00
ATOM	196	O10	MOL	1	7.830	-5.850	-2.940	1.00	0.00
ATOM	197	O31	MOL	1	7.570	-7.050	-2.860	1.00	0.00
ATOM	198	O32	MOL	1	8.910	-5.270	-2.870	1.00	0.00
TER									
ENDMDL									

Table S2. Partial charges and GAFF atom type for evaluation of electrostatic, Lennard-Jones, and intramolecular interactions. Intramolecular bond, bond-angle, and torsional interactions were taken from the GAFF potential. Atom numbers listed in column 1 follow Table S1.

atom	partial charge (e)	GAFF atom type	
1	O1	-0.581001	o
2	C1	0.632601	c
3	O2	-0.622601	oh
4	H1	0.514501	ho
5	C2	-0.133400	c3
6	H2	0.070950	hc
7	H3	0.070950	hc
8	C3	-0.073400	c3
9	H4	0.064700	hc
10	H5	0.064700	hc
11	C4	0.026400	c3
12	H6	0.086700	hc
13	C5	-0.085550	ca
14	C6	-0.100250	ca
15	H7	0.163500	ha
16	C7	-0.085550	ca
17	C8	-0.100250	ca
18	H8	0.163500	ha
19	C9	-0.062050	ca
20	C10	0.011900	c3
21	C11	-0.062900	c3
22	C12	-0.187400	c3
23	C13	0.917602	c
24	O3	-0.869051	o
25	O4	-0.869051	o
26	H9	0.032700	hc
27	H10	0.032700	hc
28	H11	0.055450	hc
29	H12	0.055450	hc
30	H13	0.096200	hc
31	C14	-0.062050	ca
32	C15	-0.100250	ca
33	H14	0.163500	ha
34	C16	-0.085550	ca
35	C17	0.026400	c3
36	H15	0.086700	hc
37	C18	-0.073400	c3
38	H16	0.064700	hc
39	C19	-0.133400	c3
40	H17	0.070950	hc
41	H18	0.070950	hc
42	C20	0.632601	c
43	O5	-0.581001	o
44	O6	-0.622601	oh
45	H19	0.514501	ho
46	H20	0.064700	hc
47	C21	-0.085550	ca

48	C22	-0.100250	ca
49	H21	0.163500	ha
50	C23	-0.062050	ca
51	C24	0.011900	c3
52	H22	0.096200	hc
53	C25	-0.062900	c3
54	H23	0.055450	hc
55	C26	-0.187400	c3
56	H24	0.032700	hc
57	H25	0.032700	hc
58	C27	0.917602	c
59	O7	-0.869051	o
60	O8	-0.869051	o
61	H26	0.055450	hc
62	C28	-0.062050	ca
63	C29	0.081600	ca
64	O9	-0.332900	os
65	C30	-0.153500	ca
66	H27	0.157000	ha
67	C31	0.077850	ca
68	O10	-0.338400	os
69	C32	0.370200	c3
70	H28	0.069700	h2
71	O11	-0.338400	os
72	C33	0.077850	ca
73	C34	-0.153500	ca
74	H29	0.157000	ha
75	C35	0.081600	ca
76	O12	-0.332900	os
77	C36	0.370200	c3
78	H30	0.066700	h2
79	O13	-0.332900	os
80	C37	0.081600	ca
81	C38	-0.153500	ca
82	H31	0.157000	ha
83	C39	0.077850	ca
84	O14	-0.338400	os
85	C40	0.370200	c3
86	H32	0.069700	h2
87	O15	-0.338400	os
88	C41	0.077850	ca
89	C42	-0.153500	ca
90	H33	0.157000	ha
91	C43	0.081600	ca
92	O16	-0.332900	os
93	C44	0.370200	c3
94	H34	0.066700	h2
95	C45	-0.032300	ca
96	C46	-0.190250	ca
97	H35	0.164500	ha
98	C47	-0.190250	ca
99	H36	0.164500	ha
100	C48	0.147600	ca
101	O17	-0.262450	os

102	C49	-0.196000	ca
103	H37	0.150000	ha
104	C50	0.147600	ca
105	O18	-0.262450	os
106	C51	0.062350	ca
107	C52	-0.099000	ca
108	C53	-0.119600	ca
109	C54	-0.100500	ca
110	H38	0.166500	ha
111	C55	0.911451	c
112	O19	-0.837926	o
113	O20	-0.837926	o
114	H39	0.167250	ha
115	C56	-0.114050	ca
116	C57	-0.050800	c3
117	H40	0.046367	hc
118	H41	0.046367	hc
119	H42	0.046367	hc
120	C58	0.061600	ca
121	O21	-0.262700	os
122	C59	0.148350	ca
123	C60	-0.196500	ca
124	H43	0.151000	ha
125	C61	-0.191000	ca
126	H44	0.163750	ha
127	C62	-0.034800	ca
128	C63	-0.191000	ca
129	H45	0.163750	ha
130	C64	0.148350	ca
131	O22	-0.262700	os
132	C65	0.061600	ca
133	C66	-0.100500	ca
134	C67	-0.119600	ca
135	C68	-0.099000	ca
136	H46	0.167250	ha
137	C69	0.911451	c
138	O23	-0.837926	o
139	O24	-0.837926	o
140	H47	0.166500	ha
141	C70	-0.114050	ca
142	C71	-0.050800	c3
143	H48	0.046367	hc
144	H49	0.046367	hc
145	H50	0.046367	hc
146	C72	0.062350	ca
147	O25	-0.262450	os
148	C73	0.147600	ca
149	C74	-0.196000	ca
150	H51	0.150000	ha
151	C75	-0.190250	ca
152	H52	0.164500	ha
153	C76	-0.032300	ca
154	C77	-0.190250	ca
155	H53	0.164500	ha

156	C78	0.147600	ca
157	O26	-0.262450	os
158	C79	0.062350	ca
159	C80	-0.099000	ca
160	C81	-0.119600	ca
161	C82	-0.100500	ca
162	H54	0.166500	ha
163	C83	0.911451	c
164	O27	-0.837926	o
165	O28	-0.837926	o
166	H55	0.167250	ha
167	C84	-0.114050	ca
168	C85	-0.050800	c3
169	H56	0.046367	hc
170	H57	0.046367	hc
171	H58	0.046367	hc
172	C86	0.061600	ca
173	O29	-0.262700	os
174	C87	0.148350	ca
175	C88	-0.196500	ca
176	H59	0.151000	ha
177	C89	-0.191000	ca
178	H60	0.163750	ha
179	C90	-0.034800	ca
180	C91	-0.191000	ca
181	H61	0.163750	ha
182	C92	0.148350	ca
183	O30	-0.262700	os
184	C93	0.061600	ca
185	C94	-0.100500	ca
186	H62	0.166500	ha
187	C95	-0.114050	ca
188	C96	-0.050800	c3
189	H63	0.046367	hc
190	H64	0.046367	hc
191	H65	0.046367	hc
192	C97	0.062350	ca
193	C98	-0.099000	ca
194	H66	0.167250	ha
195	C99	-0.119600	ca
196	OC10	0.911451	c
197	O31	-0.837926	o
198	O32	-0.837926	o

References

1. M. J. Abraham, T. Murtola, R. Schulz, S. Páll, J. C. Smith, B. Hess and E. Lindahl, *SoftwareX*, 2015, **1-2**, 19-25.
2. H. W. Horn, W. C. Swope, J. W. Pitera, J. D. Madura, T. J. Dick, G. L. Hura and T. Head-Gordon, *J. Chem. Phys.*, 2004, **120**, 9665-9678.
3. J. Wang, R. M. Wolf, J. W. Caldwell, P. A. Kollman and D. A. Case, *J. Comput. Chem.*, 2004, **25**, 1157-1174.
4. A. W. Sousa da Silva and W. F. Vranken, *BMC Research Notes*, 2012, **5**, 367.
5. A. Jakalian, D. B. Jack and C. I. Bayly, *J. Comput. Chem.*, 2002, **23**, 1623-1641.
6. J. Ewell, B. C. Gibb and S. W. Rick, *J. Phys. Chem. B*, 2008, **112**, 10272-10279.
7. S. W. I. Siu, K. Pluhackova and R. A. Bockmann, *J. Chem. Theory Comput.*, 2012, **8**, 1459-1470.
8. M. P. Allen and D. J. Tildesley, *Computer simulation of liquids*, Oxford University Press, Oxford, UK, 1987.
9. T. Darden, D. York and L. Pedersen, *J. Chem. Phys.*, 1993, **98**, 10089-10092.
10. S. Nosé, *J. Chem. Phys.*, 1984, **81**, 511-519; W. G. Hoover, *Phys. Rev. A*, 1985, **31**, 1695-1697.
11. M. Parrinello and A. Rahman, *J. Appl. Phys.*, 1981, **52**, 7182-7190.
12. B. Hess, H. Bekker, H. J. C. Berendsen and J. Fraaije, *J. Comput. Chem.*, 1997, **18**, 1463-1472.
13. S. Miyamoto and P. A. Kollman, *J. Comput. Chem.*, 1992, **13**, 952-962.
14. M. R. Shirts and J. D. Chodera, *J. Chem. Phys.*, 2008, **129**, 10.